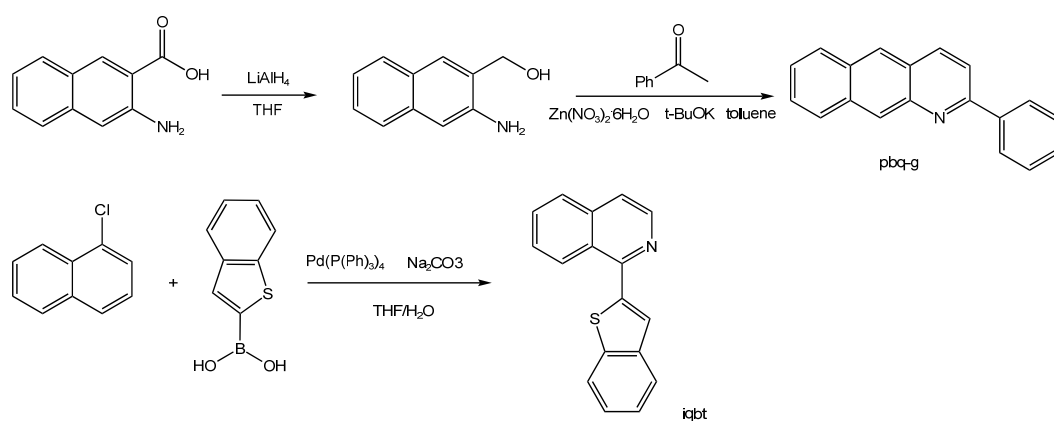


Supporting Information

Two near-infrared phosphorescent iridium(III) complexes for detection of GSH and photodynamic therapy

Rui Tu, Jie Liu, Weibin Chen, Fengfu Fu, Mei-Jin Li*



Scheme S1 Synthetic route to pbq-g, iqbt

† These authors contributed equally to this work.

* Corresponding author. E-mail address: mjli@fzu.edu.cn

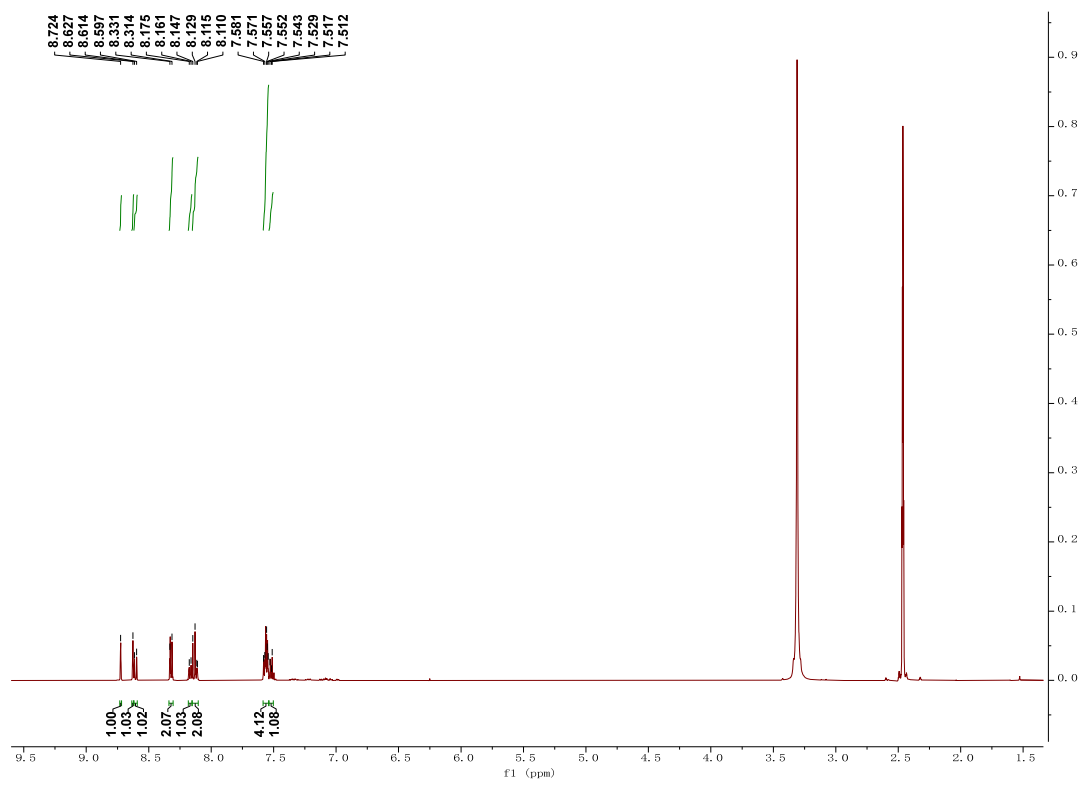


Fig.S1 ¹H NMR (400 MHz, DMSO-*d*₆) spectrum of pbq-g

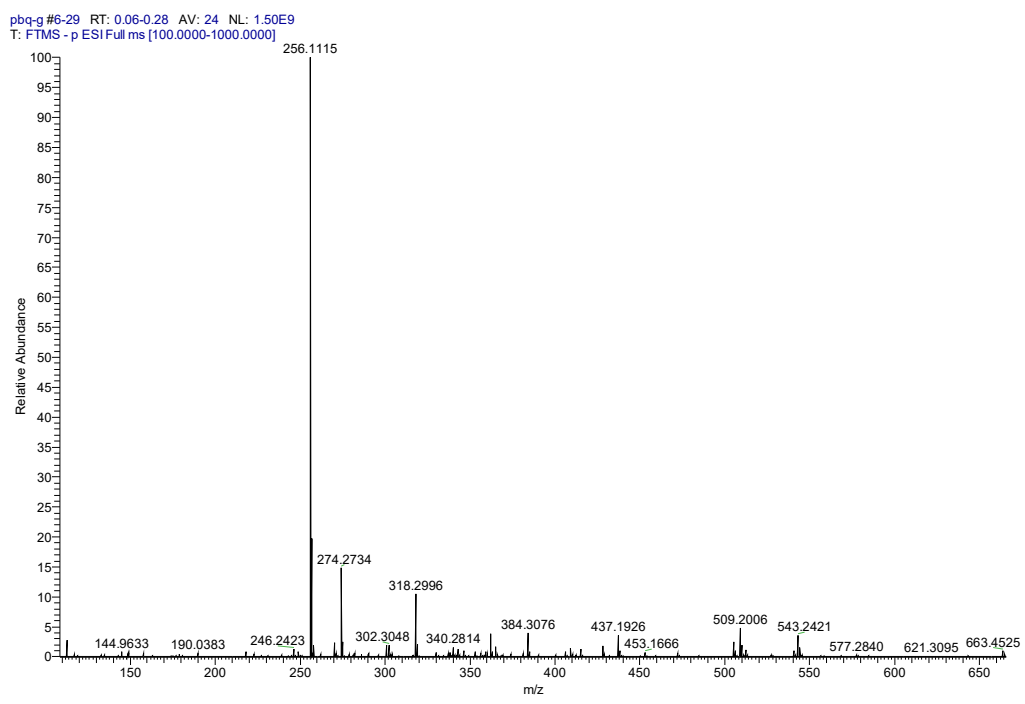


Fig.S2 ESI-MS of pbq-g: $m/z=256.1115 \{M+H\}^+$

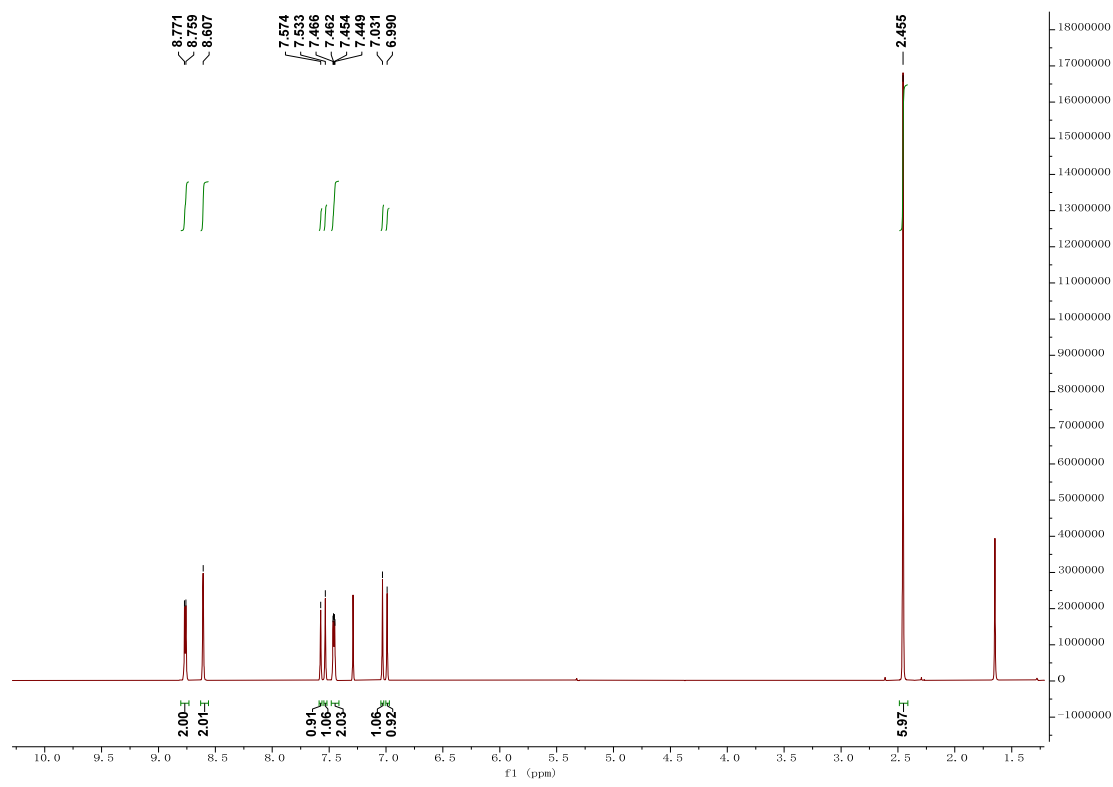


Fig.S3 ¹H NMR (400 MHz, CDCl₃) spectrum of L

byp-ace #12-21 RT: 0.12-0.21 AV: 10 NL: 1.93E9
 T: FTMS - p ESI Full ms [200.0000-2000.0000]

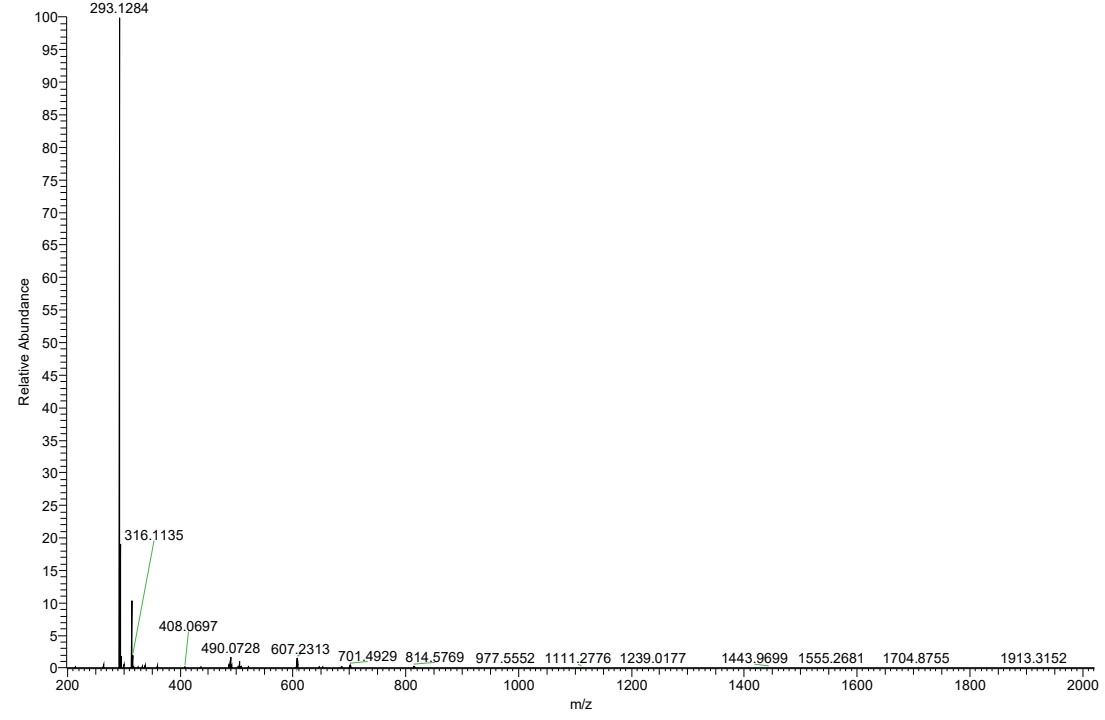


Fig.S4 ESI-MS of L: m/z=293.1284 {M+H}⁺

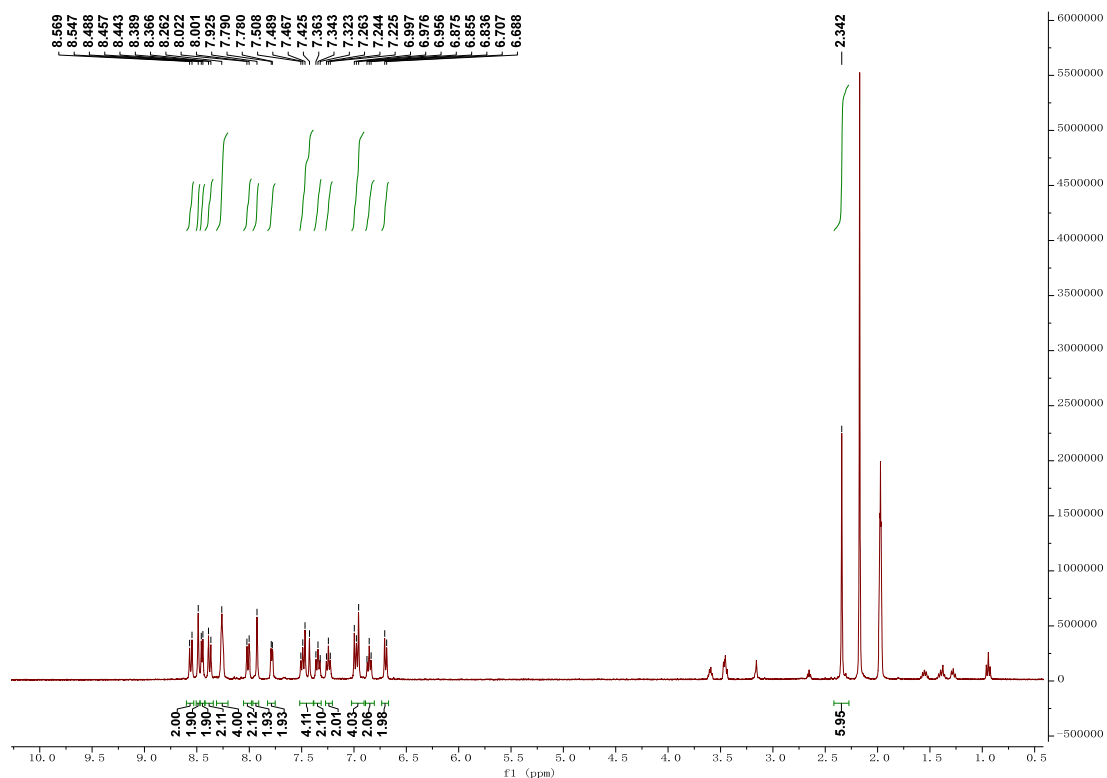


Fig.S5(a) ^1H NMR (400 MHz, CD_3CN) spectrum of $[\text{Ir}(\text{pbq-g})_2\text{L}]\text{PF}_6$

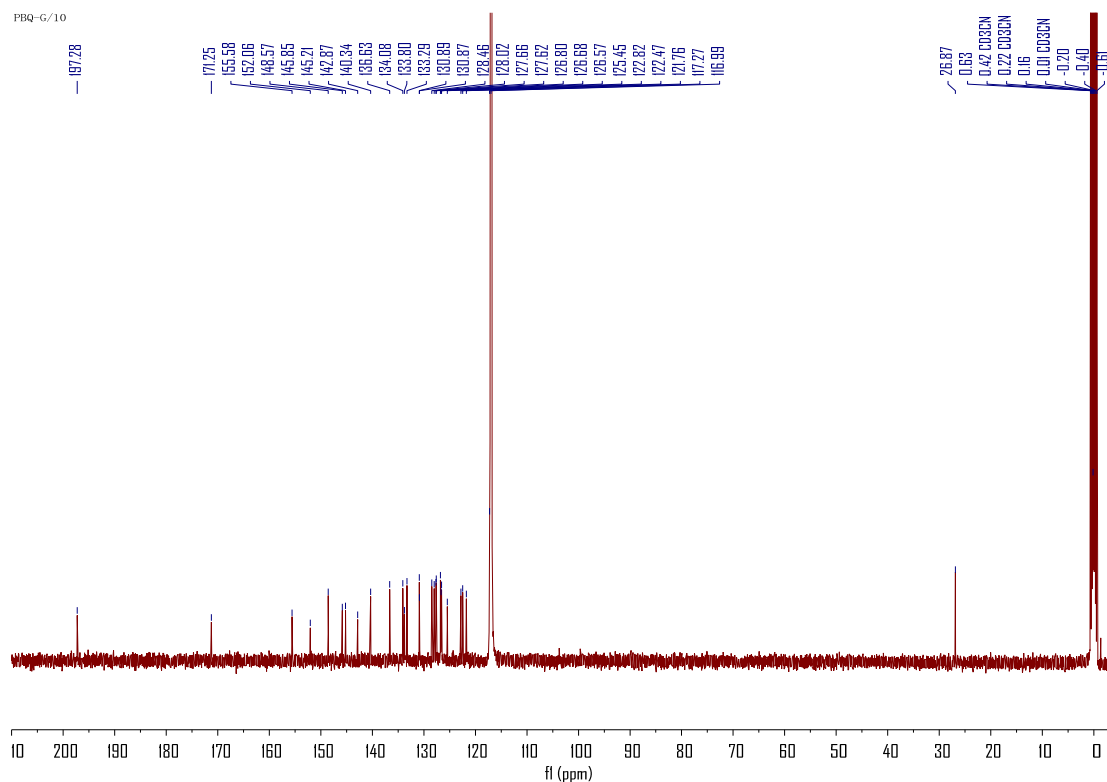


Fig.S5(b) ^{13}C NMR (101 MHz, CD_3CN) spectrum of $[\text{Ir}(\text{pbq-g})_2\text{L}]\text{PF}_6$

[Ir(pbq-g)₂byp-acePF₆ #27-45 RT: 0.18-0.27 AV: 19 NL: 1.56E8
T: FTMS + p ESI Full ms [200.0000-2000.0000]

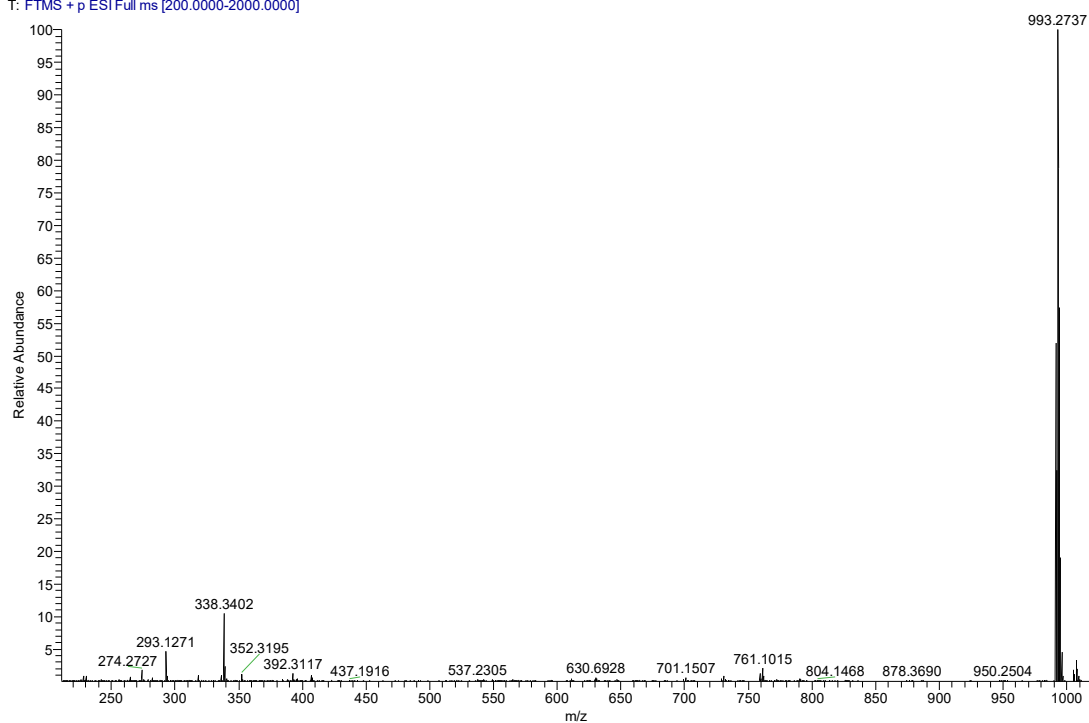


Fig.S6 ESI-MS of [Ir(pbq-g)₂L]PF₆: m/z=993.2737 {M-PF₆}⁺

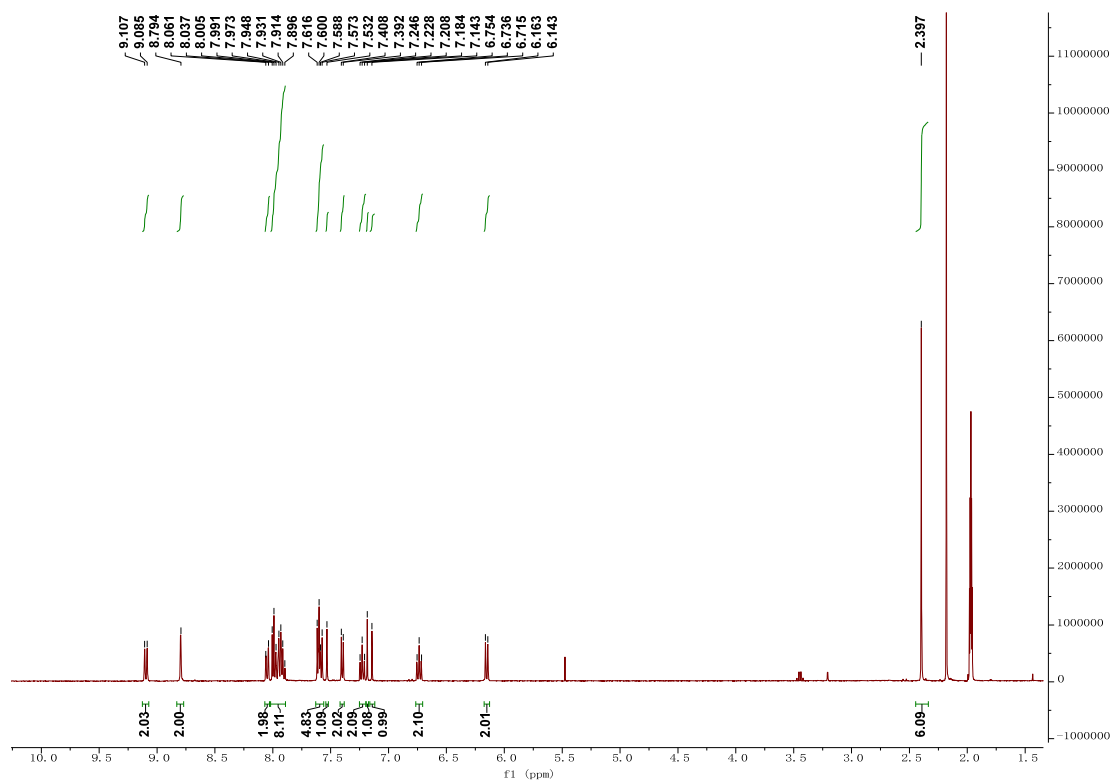


Fig.S7(a) ¹H NMR (400 MHz, CD₃CN) spectrum of [Ir(iqbt)₂L]PF₆

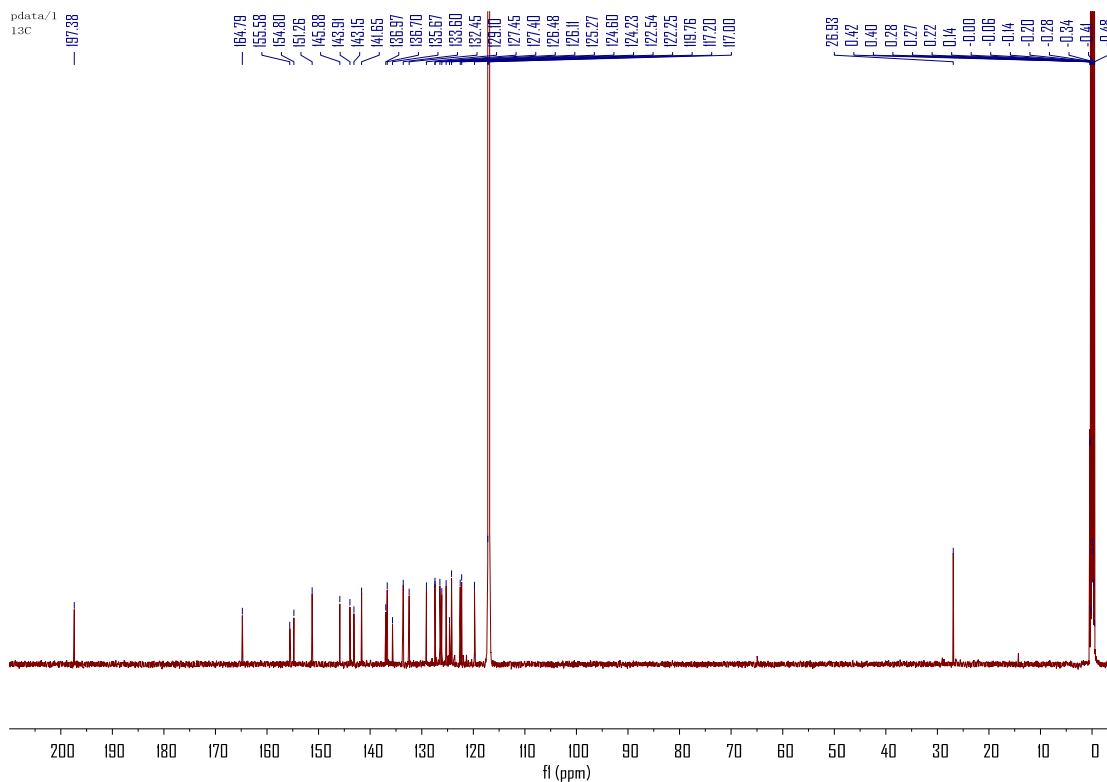


Fig.S7(b) ^{13}C NMR (151 MHz, CD_3CN) spectrum of $[\text{Ir}(\text{iqbt})_2\text{L}]\text{PF}_6$

Ir(iqbt)2bpy-acePF6 #8-45 RT: 0.06-0.27 AV: 38 NL: 1.32E8
T: FTMS + p ESI Full ms [200.0000-2000.0000]

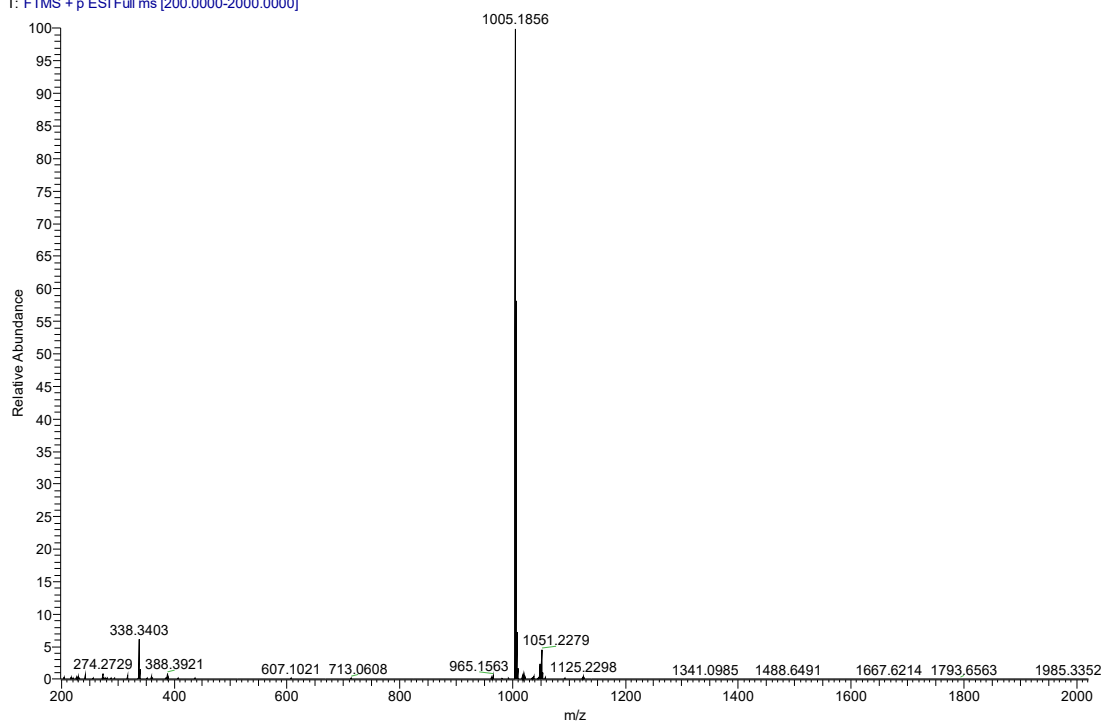


Fig.S8 ESI-MS of $[\text{Ir}(\text{iqbt})_2\text{L}]\text{PF}_6$: $m/z=1005.1856 \{M-\text{PF}_6\}^+$

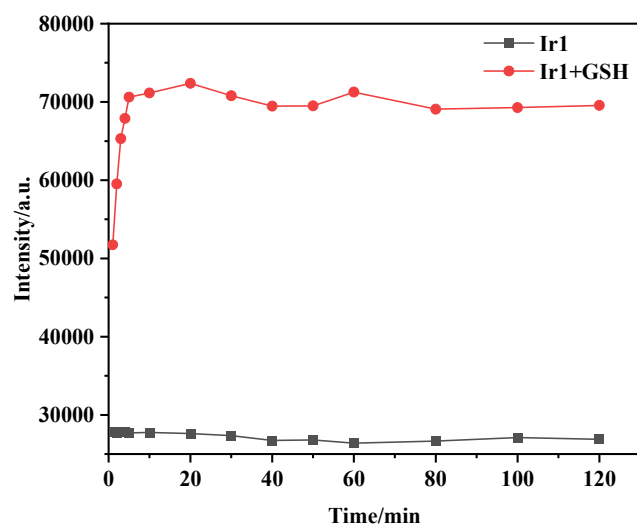


Fig.S9 Change of PL intensity of **Ir1**(10 μ M) and **Ir1**(10 μ M) +GSH (100 μ M) with different time. λ_{ex} =450 nm, λ_{em} =704 nm.

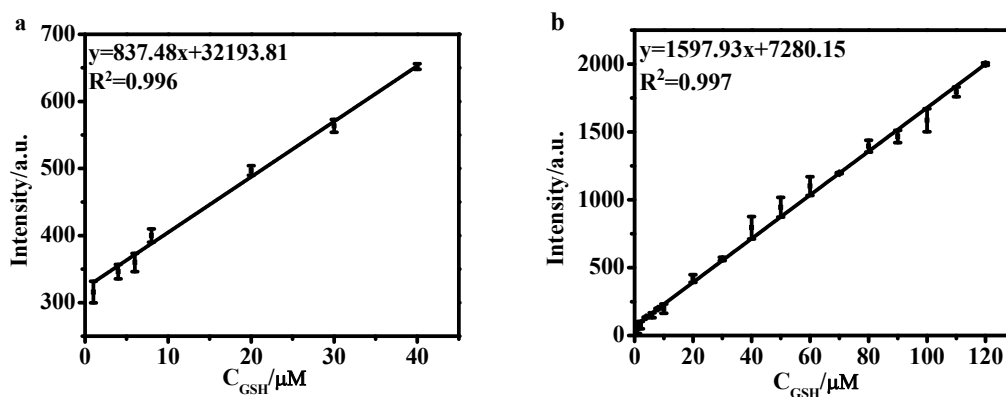


Fig.S10 A plot of the luminescence intensity of complexes as a function of GSH concentration for (a) **Ir1**+GSH(1.0-40 μ M) (λ_{ex} =450 nm, λ_{em} =704 nm) in DMSO-phosphate buffer solution (10 mM, pH = 7.4, 2:3, v/v) and (b) **Ir2**+GSH (0.5-120 μ M) (λ_{ex} =520 nm, λ_{em} =684 nm) in DMSO-phosphate buffer solution (10 mM, pH = 7.4, 4:1, v/v)

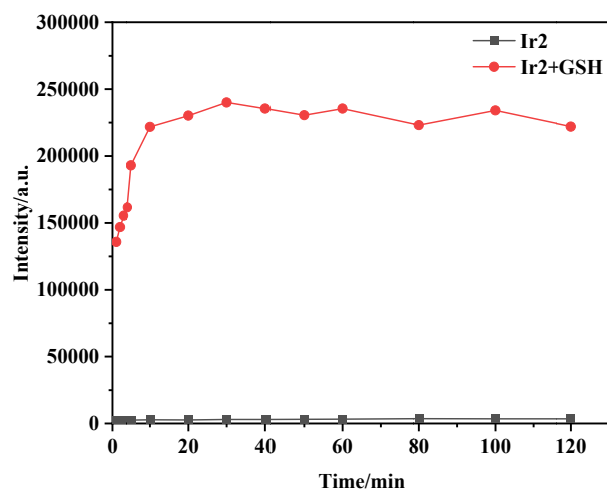


Fig.S11 Change of PL intensity of **Ir2**(10 μ M) and **Ir2**(10 μ M) + GSH(150 μ M) with different time. λ_{ex} =520 nm, λ_{em} =684 nm.

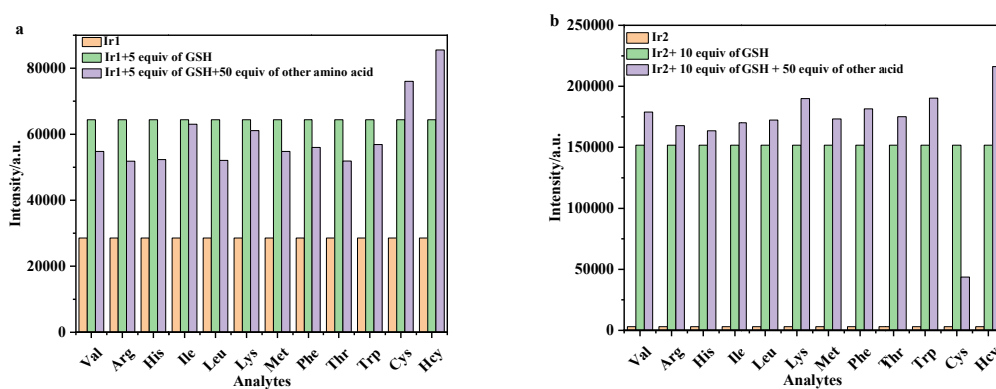


Fig.S12 (a) The behavior of **Ir1** (10 μ M) toward GSH and other related analytes in DMSO-PBS buffer solution (10 mM, pH = 7.4, 2:3, v/v). λ_{ex} = 450 nm, λ_{em} = 704 nm; (b) The behavior of **Ir2** (10 μ M) toward GSH and other related analytes in DMSO-PBS buffer solution (10 mM, pH = 7.4, 4:1, v/v). λ_{ex} = 520 nm, λ_{em} = 684 nm

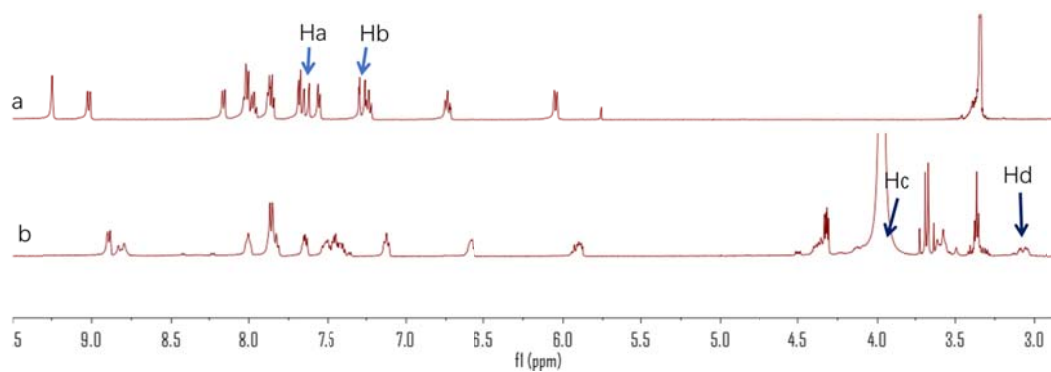


Fig.S13 ^1H NMR spectra of (a) **Ir2** and (b) **Ir2** + GSH in DMSO- D_2O solution (4:1, v/v)

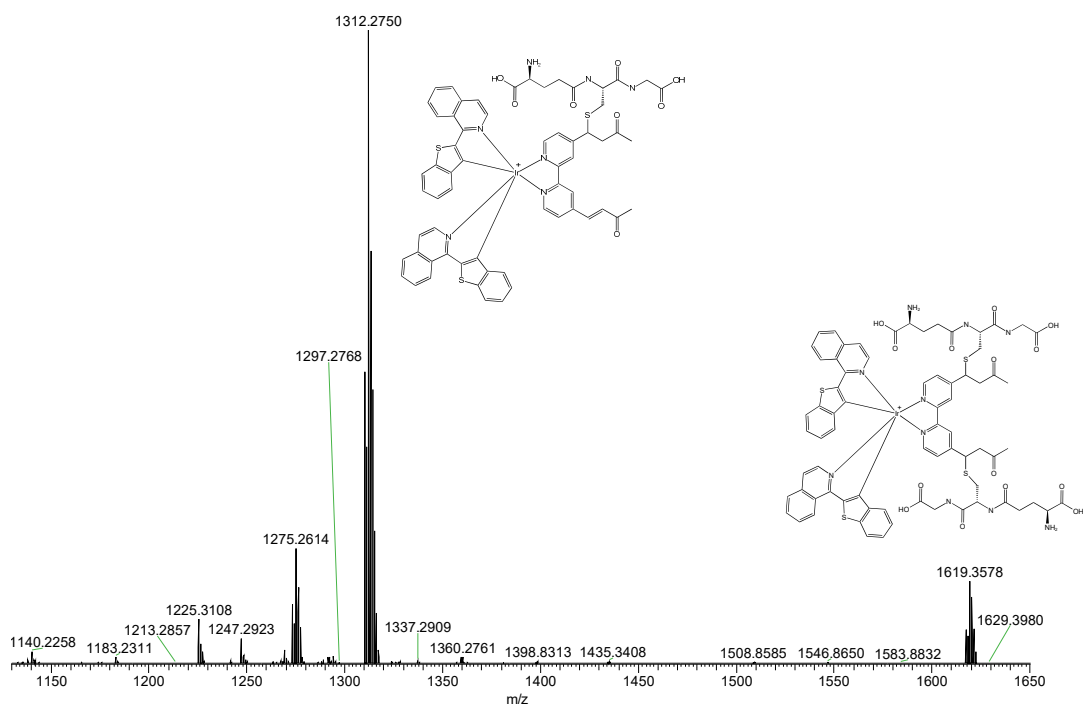


Fig.S14 ESI-MS of Ir2 + GSH

Table S1 Coordination probes of GSH detection as reporter

Structure	$\lambda_{ex}/$ nm	$\lambda_{em}/$ nm	Response time	LOD	Linear range	Test condition	Ref
	405	704	6min		0-40 μ M	DMSO:PBS(pH 7.4, v/v, 1:9)	1
	400	595		2.34 μ M	0-40 μ M	CH ₃ CN:HEPES (10 mM, pH 7.4, v/v,1:1)	2
	480	628	15min	0.138 μ M	0-16 μ M	Tris-HCl buffer (50 mM pH 7.4)	3
	458	625		1 μ M	5-90 μ M	ethanol:HEPES buffer (50 mM pH 7.2, v/v,1:4)	4

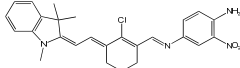
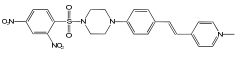
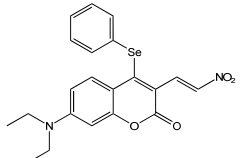
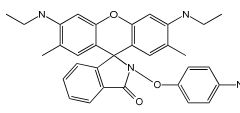
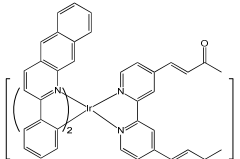
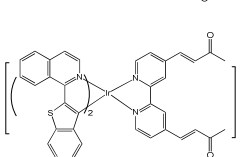
	653	720	25s	0.25 μM	0-16 μM	DMSO:HEPES (10 mM, pH 7.4, v/v, 1:10)	5
		586	20min	0.25 μM	0-20 μM	PBS (10 mM, pH 7.4)	6
	480	542	20min	0.83 μM	0-80 μM	DMSO:PBS (pH 7.4, v/v,1:9)	7
	510	557	3s	49.6 μM	0-5m M	Ethanol:Tris-H Cl (10 mM, pH 7.45, v/v, 5:5)	8
	450	704	5min	0.38 μM	1.0-40 μM	DMSO:PBS(pH 7.4, v/v, 2:3)	This work
	520	684	10min	0.17 μM	0.5-12 0 μM	DMSO:PBS(pH 7.4, v/v, 4:1)	This work

Table S2 Complex **Ir2** and **Ir2-GSH** photophysical properties data in DMSO

Complex	λ_{abs} ($\epsilon / 10^4 \text{ dm}^3 \text{ mol}^{-1} \text{ cm}^{-1}$)	λ_{ex} /nm	λ_{em} /nm	t /ns	Φ
Ir2-GSH	259(3.9), 287(3.1), 309(3.1), 362(1.9), 482(0.8)	494	684, 748	412	0.014
Ir2	281(4.2), 308(3.9), 345(2.6), 366(2.3), 489(0.9)	497	686, 750	206	0.002

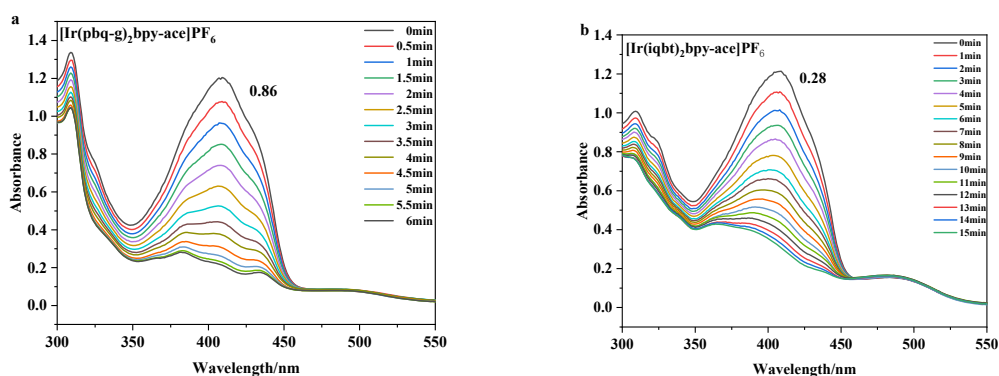


Fig.S15 UV-vis absorption spectra of a mixture of DPBF (50 μM) and (a) **Ir1** (10 μM); (b) **Ir2** (10 μM) in acetonitrile under irradiation at 450nm.

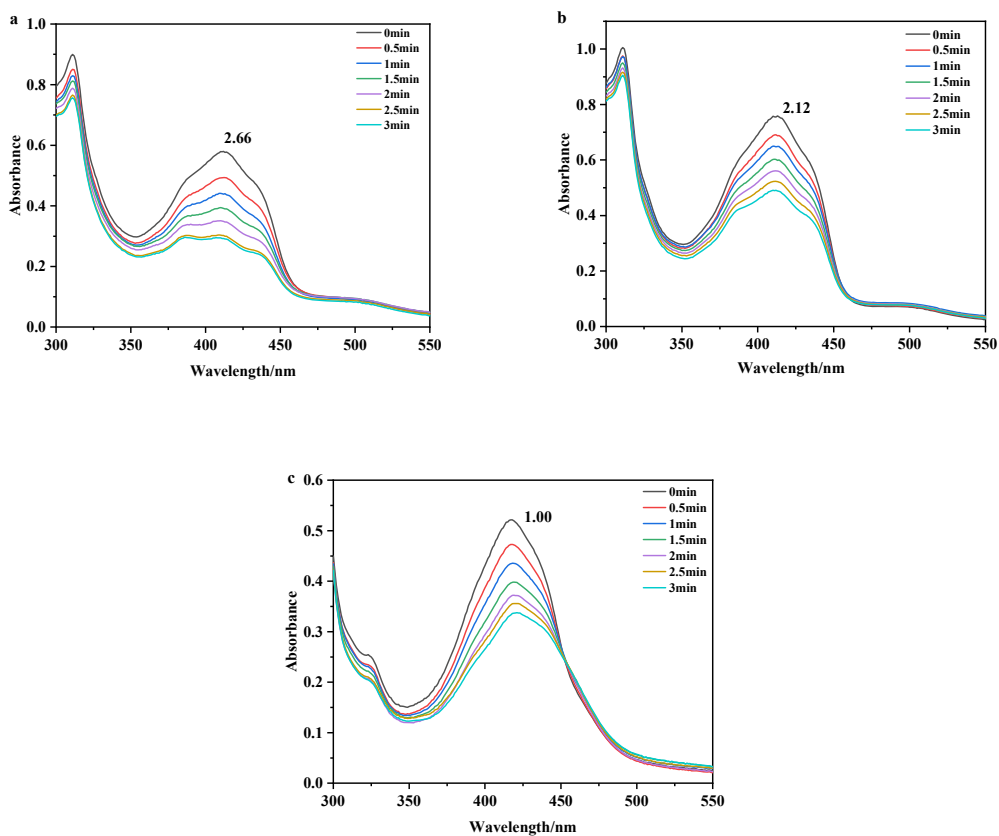


Fig.S16 The absorption spectra of a mixture of DPBF (50 μM) and (a) **Ir1**(10 μM); (b) **Ir1** (10 μM) +5 equiv. of GSH; (c) **Ru(bpy)₃²⁺** (10 μM) in DMSO-PBS buffer solution (10 mM, pH = 7.4, 2:3, v/v) under irradiation at 450nm.

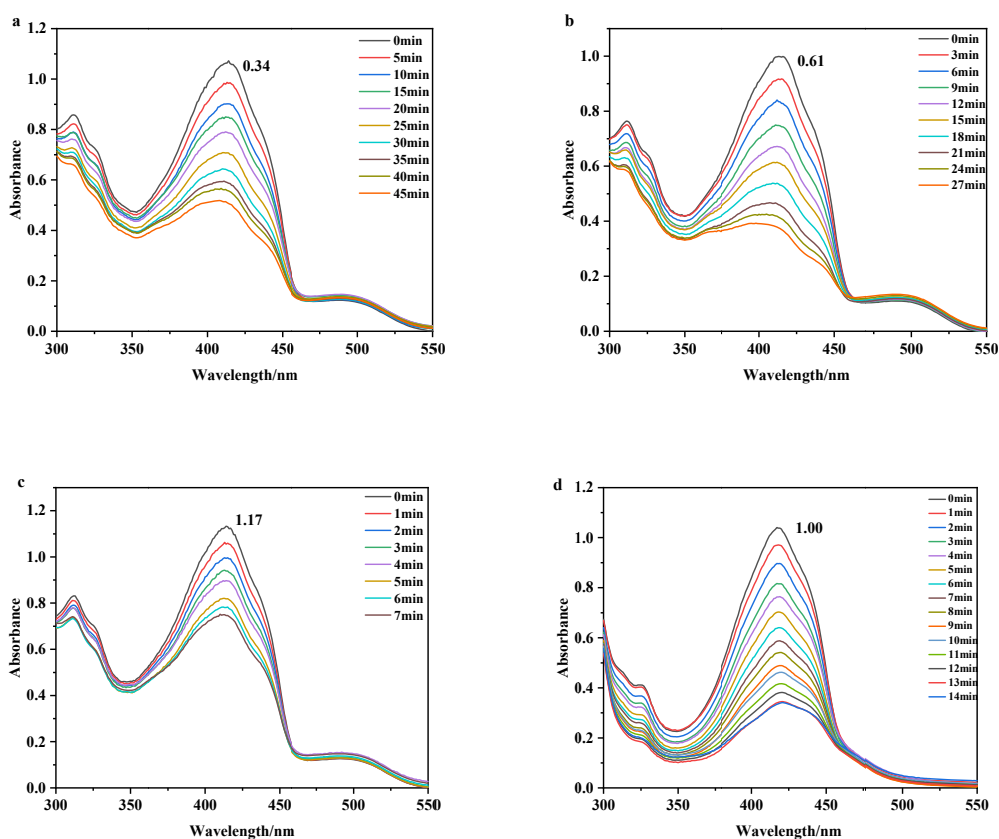


Fig.S17 The absorption spectra of a mixture of DPBF (50 μ M) and (a) **Ir2** (10 μ M); (b) **Ir2** (10 μ M) +10 equiv. of GSH; (c) **Ir2** (10 μ M) +20 equiv. of GSH; (d) $\text{Ru}(\text{bpy})_3^{2+}$ (10 μ M) in DMSO-PBS buffer solution (10 mM, pH = 7.4, 4:1, v/v) under irradiation at 450nm.

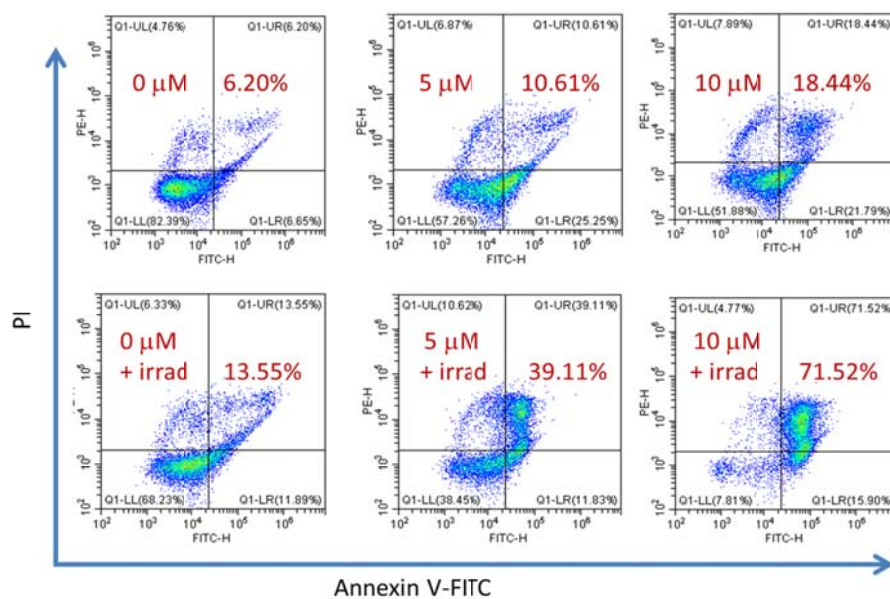


Fig. S18 Complex mediated cells apoptosis in dose-dependent and irradiation-dependent manner. Cells were treated with different dose of **Ir2** for 10 h without or under irradiation for 8min with 450nm light. Then the percentage of apoptosis cells was analyzed with flow cytometry.

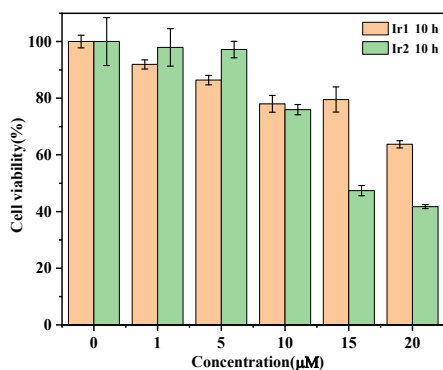


Fig.S19 Viability of HeLa cells in the presence of different concentrations of iridium(III) complexes

References

- [1]. W. Wu, X. Liao, Y. Chen, L. Ji, and H. Chao. *Anal. Chem.*, 2021, 93, 8062-8070.
- [2] H. S. No, T. Kim, J. I Hong, *Sensor. Actuat. B. Chem*,2021,342,129868.
- [3] C. L. Liu, J. P. Liu, W. Z. Zhang, Y. L. Wang, Q. Liu, B. Song , J. L. Yuan and R. Zhang, *Adv. Sci.*, 2020, 7,2000458.
- [4] Z. Q. Ye, Q. K. Gao, X. An, B. Song, and J. L. Yuan, *Dalton Tran.*, 2015, 44, 8278-8283.
- [5] K. P. Wang, G. Nie, S. Q. Ran, H. L. Wang, X. Q. Liu, Z.M. Zheng and Y. Zhang, *Dyes Pigm.*, 2020, 172, 107837.
- [6] H. Y. Wang, L. Zhang, X. Jin, P. J. Tian and X. J. Ding, *RSC Adv.*, 2022,12 ,33922.
- [7] X. G. Chen, Y. Mei, Q.H Song, *Dyes Pigm.*,2022, 110312.
- [8] Z.L. Zhou, P. J. Li, Z. H. Liu, C. Y. Wu, Y. Y. Zhang and H. T. Li, *Talanta*, 2022,243, 123364.